Monthly Notices
of the
ROYAL ASTRONOMICAL SOCIETY

MNRAS **465,** 3693–3707 (2017)
Advance Access publication 2016 November 22

doi:10.1093/mnras/stw3005

WASP-South transiting exoplanets: WASP-130b, WASP-131b, WASP-132b, WASP-139b, WASP-140b, WASP-141b and WASP-142b

C. Hellier,[1]★ D. R. Anderson,[1] A. Collier Cameron,[2] L. Delrez,[3] M. Gillon,[3] E. Jehin,[3] M. Lendl,[4,5] P. F. L. Maxted,[1] M. Neveu-VanMalle,[5,6] F. Pepe,[5] D. Pollacco,[7] D. Queloz,[6] D. Ségransan,[5] B. Smalley,[1] J. Southworth,[1] A. H. M. J. Triaud,[5,8] S. Udry,[5] T. Wagg[1] and R. G. West[7]

[1]*Astrophysics Group, Keele University, Staffordshire ST5 5BG, UK*
[2]*SUPA, School of Physics and Astronomy, University of St. Andrews, North Haugh, Fife KY16 9SS, UK*
[3]*Institut d'Astrophysique et de Géophysique, Université de Liège, Allée du 6 Août, 17, Bat. B5C, Liège 1, Belgium*
[4]*Space Research Institute, Austrian Academy of Sciences, Schmiedlstr. 6, A-8042 Graz, Austria*
[5]*Observatoire Astronomique de l'Université de Genève 51 ch. des Maillettes, CH-1290 Sauverny, Switzerland*
[6]*Cavendish Laboratory, J J Thomson Avenue, Cambridge CB3 0HE, UK*
[7]*Department of Physics, University of Warwick, Gibbet Hill Road, Coventry CV4 7AL, UK*
[8]*Institute of Astronomy, University of Cambridge, Cambridge CB3 0HA, UK*

Accepted 2016 November 17. Received 2016 November 15; in original form 2016 April 15

ABSTRACT

We describe seven exoplanets transiting stars of brightness $V = 10.1$–12.4. WASP-130b is a 'warm Jupiter' having an orbital period of 11.6 d around a metal-rich G6 star. Its mass and radius (1.23 ± 0.04 M_{Jup} and 0.89 ± 0.03 R_{Jup}) support the trend that warm Jupiters have smaller radii than hot Jupiters. WASP-131b is a bloated Saturn-mass planet (0.27 M_{Jup} and 1.22 R_{Jup}). Its large scaleheight and bright ($V = 10.1$) host star make it a good target for atmospheric characterization. WASP-132b (0.41 M_{Jup} and 0.87 R_{Jup}) is among the least irradiated and coolest of WASP planets, having a 7.1-d orbit around a K4 star. WASP-139b is a 'super-Neptune' akin to HATS-7b and HATS-8b, being the lowest mass planet yet found by WASP (0.12 M_{Jup} and 0.80 R_{Jup}). The metal-rich K0 host star appears to be anomalously dense, akin to HAT-P-11. WASP-140b is a 2.4-M_{Jup} planet in an eccentric ($e = 0.047 \pm 0.004$) 2.2-d orbit. The planet's radius is large (1.4 R_{Jup}), but uncertain owing to the grazing transit ($b = 0.93$). The 10.4-d rotation period of the K0 host star suggests a young age, and the time-scale for tidal circularization is likely to be the lowest of all known eccentric hot Jupiters. WASP-141b (2.7 M_{Jup}, 1.2 R_{Jup} and $P = 3.3$ d) and WASP-142b (0.84 M_{Jup}, 1.53 R_{Jup} and $P = 2.1$ d) are typical hot Jupiters orbiting metal-rich F stars. We show that the period distribution within the hot-Jupiter bulge does not depend on the metallicity of the host star.

Key words: stars: individual (WASP-130, WASP-131, WASP-132, WASP-139, WASP-140, WASP-141, WASP-142) – planetary systems.

1 INTRODUCTION

The WASP survey continues to be a productive means of finding giant planets transiting relatively bright stars. WASP discoveries are often prime targets for further study. For example Sing et al. (2016) devoted 125 orbits of *Hubble Space Telescope* time to exoplanet atmospheres, of which six out of eight targets were WASP planets. Similarly, Stevenson et al. (2016) propose 12 planets as 'community targets' for atmospheric characterization in Cycle 1 of the *James Webb Space Telescope*, of which seven are WASP planets. Ongoing discoveries also increase the census of closely orbiting giant planets, and continue to find planets with novel characteristics.

Here, we report seven new transiting giant planets discovered by the WASP-South survey instrument in conjunction with the Euler/CORALIE spectrograph and the robotic TRAPPIST photometer. With 200-mm lenses the eight WASP-South cameras can cover up to half the available sky per year (south of declination $+08^\circ$ and avoiding the crowded galactic plane). This means that the data that led to the current discoveries, accumulated from 2006 May

★ E-mail: c.hellier@keele.ac.uk

Table 1. Observations.

Facility	Date	Notes
WASP-130		
WASP-South	2006 May–2012 June	28 400 points
CORALIE	2014 February–2016 March	27 RVs
EulerCAM	2014 May 04	Gunn *r* filter
EulerCAM	2014 May 27	Gunn *r* filter
TRAPPIST	2014 May 27	z' band
TRAPPIST	2015 February 05	z' band
TRAPPIST	2015 April 27	z' band
EulerCAM	2015 April 27	Gunn *r* filter
WASP-131		
WASP-South	2006 May–2012 June	23 300 points
CORALIE	2014 February–2016 March	23 RVs
TRAPPIST	2014 April 22	z band
EulerCAM	2014 April 22	Gunn *r* filter
EulerCAM	2015 March 02	I_c filter
EulerCAM	2015 April 03	I_c filter
TRAPPIST	2015 April 19	z band
TRAPPIST	2015 June 06	z' band
WASP-132		
WASP-South	2006 May–2012 June	23 300 points
CORALIE	2014 March–2016 March	36 RVs
TRAPPIST	2014 May 05	$I+z$ band
WASP-139		
WASP-South	2006 May–2012 June	21 000 points
CORALIE	2008 October–2015 December	24 RVs
HARPS	2014 September–2015 January	27 RVs
TRAPPIST	2014 August 06	$I+z$ band
TRAPPIST	2015 September 07	$I+z$ band
EulerCAM	2015 September 07	*NGTS* filter
WASP-140		
WASP-South	2006 August–2012 January	31 300 points
CORALIE	2014 September–2015 December	23 RVs
TRAPPIST	2014 October 12	z' band
TRAPPIST	2014 November 28	z' band
TRAPPIST	2014 December 07	z' band
EulerCAM	2015 September 01	I_c filter
WASP-141		
WASP-South	2006 September–2012 February	21 400 points
CORALIE	2014 October–2015 December	18 RVs
EulerCAM	2014 December 17	*NGTS* filter
TRAPPIST	2015 January 19	$I+z$ band
TRAPPIST	2015 December 26	$I+z$ band
WASP-142		
WASP-South	2006 May–2012 May	47 300 points
CORALIE	2014 October–2016 February	16 RVs
TRAPPIST	2014 May 26	Blue-block
EulerCAM	2014 December 13	I_c filter
EulerCAM	2015 March 01	I_c filter
TRAPPIST	2015 April 03	Blue-block

to 2012 June, typically includes three seasons of coverage, or more where pointings overlap. Combining multiple years of observation gives sensitivity to longer orbital periods, and this batch of planets includes the longest period WASP discovery yet, a 'warm Jupiter' at 11.6 d.

2 OBSERVATIONS

Since the processes and techniques used here are a continuation of those from other recent WASP-South discovery papers (e.g. Anderson et al. 2014; Hellier et al. 2014; Maxted et al. 2016), we describe them briefly. The WASP camera arrays (Pollacco et al. 2006) tile fields of $7.8^\circ \times 7.8^\circ$ with a typical cadence of 10 min, using 200 mm *f*/1.8 lenses backed by 2k×2k Peltier-cooled CCDs. Using transit-search algorithms (Collier Cameron et al. 2007b) we trawl the accumulated multi-year light curves for planet candidates, which are then passed to the 1.2-m Euler/CORALIE spectrograph (e.g. Triaud et al. 2013), for radial-velocity observations, and to the robotic 0.6-m TRAPPIST photometer, which resolves candidates which are blended in WASP's large, 14 arcsec, pixels. TRAPPIST (e.g. Gillon et al. 2013) and EulerCAM (e.g. Lendl et al. 2012) then obtain higher quality photometry of newly confirmed planets. For one system reported here, WASP-139, we have also obtained radial velocities using the HARPS spectrometer on the ESO 3.6 m (Mayor et al. 2003). A list of our observations is given in Table 1 while the radial velocities are listed in Table A1.

3 THE HOST STARS

We used the CORALIE spectra to estimate spectral parameters of the host stars using the methods described in Doyle et al. (2013). We used the Hα line to estimate the effective temperature ($T_{\rm eff}$), and the Na I D and Mg I b lines as diagnostics of the surface gravity ($\log g$). The iron abundances were determined from equivalent-width measurements of several clean and unblended Fe I lines and are given relative to the solar value presented in Asplund et al. (2009). The quoted abundance errors include that given by the uncertainties in $T_{\rm eff}$ and $\log g$, as well as the scatter due to measurement and atomic data uncertainties. The projected rotation velocities ($v \sin i$) were determined by fitting the profiles of the Fe I lines after convolving with the CORALIE instrumental resolution ($R = 55\,000$) and a macroturbulent velocity adopted from the calibration of Doyle et al. (2014).

The parameters obtained from the analysis are given in Tables 2–8. Gyrochronological age estimates are given for three stars, derived from the measured $v\sin i$ and compared to values in Barnes (2007); for the other stars no sensible constraint is obtained. Lithium age estimates come from values in Sestito & Randich (2005). We also list proper motions from the UCAC4 catalogue (Zacharias et al. 2013).

We searched the WASP photometry of each star for rotational modulations by using a sine-wave fitting algorithm as described by Maxted et al. (2011). We estimated the significance of periodicities by subtracting the fitted transit light curve and then repeatedly and randomly permuting the nights of observation. We found a significant modulation in WASP-140 (see Section 10) and a possible modulation in WASP-132 (Section 8) and report upper limits for the other stars.

4 SYSTEM PARAMETERS

The CORALIE radial-velocity measurements (and the HARPS data for WASP-139) were combined with the WASP, EulerCAM and TRAPPIST photometry in a simultaneous Markov chain Monte Carlo (MCMC) analysis to find the system parameters. CORALIE was upgraded in 2014 November, and so we treat the RV data before and after that time as independent data sets, allowing a zero-point offset between them (the division is indicated by a short horizontal line in Table A1). For more details of our methods see Collier Cameron et al. (2007a). The limb-darkening parameters are noted in each table, and are taken from the four-parameter non-linear law of Claret (2000).

For WASP-140b, the orbital eccentricity is significant and was fitted as a free parameter. For the others we imposed a circular orbit

Table 2. System parameters for WASP-130.

1SWASP J133225.42–422831.0	
2MASS 13322543–4228309	
RA = $13^h32^m25.43^s$, Dec. = $-42°28'30.9''$ (J2000)	
V mag = 11.1	
Rotational modulation < 1 mmag (95 per cent)	
pm (RA) 7.0 ± 2.5 (Dec.) –0.7 ± 1.3 mas yr^{-1}	
Stellar parameters from spectroscopic analysis	
Spectral type	G6
$T_{\rm eff}$ (K)	5600 ± 100
log g	4.4 ± 0.1
$v \sin i$ (km s^{-1})	0.5 ± 0.5
[Fe/H]	+0.26 ± 0.10
log A(Li)	<0.4
Age (Lithium) (Gyr)	$\gtrsim$2
Distance (pc)	180 ± 30
Parameters from MCMC analysis	
P (d)	11.55098 ± 0.00001
$T_{\rm c}$ (HJD) (UTC)	245 6921.14307 ± 0.00025
T_{14} (d)	0.155 ± 0.001
$T_{12} = T_{34}$ (d)	0.018 ± 0.001
$\Delta F = R_{\rm P}^2/R_*^2$	0.00916 ± 0.00014
b	0.53 ± 0.03
i (°)	88.66 ± 0.12
K_1 (km s^{-1})	0.108 ± 0.002
γ (km s^{-1})	1.462 ± 0.002
e	0 (adopted) (<0.04 at 2σ)
$M_\star$ ($M_\odot$)	1.04 ± 0.04
$R_\star$ ($R_\odot$)	0.96 ± 0.03
log g_* (cgs)	4.49 ± 0.02
$\rho_\star$ ($\rho_\odot$)	1.18 ± 0.09
$T_{\rm eff}$ (K)	5625 ± 90
$M_{\rm P}$ ($M_{\rm Jup}$)	1.23 ± 0.04
$R_{\rm P}$ ($R_{\rm Jup}$)	0.89 ± 0.03
log $g_{\rm P}$ (cgs)	3.55 ± 0.03
$\rho_{\rm P}$ ($\rho_{\rm J}$)	1.76 ± 0.18
a (au)	0.1012 ± 0.0014
$T_{\rm P,\,A=0}$ (K)	833 ± 18
Errors are 1σ; Limb-darkening coefficients were:	
r band: a1 = 0.669, a2 = −0.400, a3 = 0.976, a4 = −0.481	
z band: a1 = 0.657, a2 = −0.454, a3 = 0.834, a4 = −0.407.	

since hot Jupiters are expected to circularize on a time-scale less than their age, and so adopting a circular orbit gives the most likely parameters (see, e.g. Anderson et al. 2012).

The fitted parameters were $T_{\rm c}$, P, ΔF, T_{14}, b, K_1, where $T_{\rm c}$ is the epoch of mid-transit, P is the orbital period, ΔF is the fractional flux-deficit that would be observed during transit in the absence of limb-darkening, T_{14} is the total transit duration (from first to fourth contact), b is the impact parameter of the planet's path across the stellar disc and K_1 is the stellar reflex velocity semi-amplitude.

The transit light curves lead directly to stellar density but one additional constraint is required to obtain stellar masses and radii, and hence full parametrization of the system. As with other recent WASP discovery papers, we compare the derived stellar density and the spectroscopic effective temperature and metallicity to a grid of stellar models, as described in Maxted, Serenelli & Southworth (2015a). We use an MCMC method to calculate the posterior distribution for the mass and age estimates of the star. The stellar models were calculated using the GARSTEC stellar evolution code (Weiss & Schlattl 2008) and the methods used to calculate the stellar model grid are described in Serenelli et al. (2013).

For each system we list the resulting parameters in Tables 2–8 and show the data and models in Figs 1–14. We generally report 1σ error bars on all quantities. For the possible effects of red noise in transit light curves and their effect on system parameters see the extensive analysis by Smith et al. (2012). We report the comparison to stellar models in Table 9, where we give the likeliest age and the 95 per cent confidence interval, and display the comparison in Fig. 15.

5 WASP-130

WASP-130 is a $V = 11.1$, G6 star with a metallicity of [Fe/H] = +0.26 ± 0.10. The transit log g_* of 4.49 ± 0.02 is consistent with the spectroscopic log g_* of 4.4 ± 0.1. The evolutionary comparison (Fig. 15) suggests an age of 0.2–7.9 Gyr (consistent with the lithium age estimate of $\gtrsim$2 Gyr).

The radial velocities show excess scatter with could be due to magnetic activity, though in this system there is no detection of a rotational modulation in the WASP data. Scatter when folded on the orbital period can also be caused by a longer term trend, but that is not the case here.

The planet, WASP-130b, has an orbital period of 11.6 d, the longest yet found by WASP-South, and is thus a 'warm Jupiter'. For comparison, the HATNet and HATSouth projects have cameras at more than one longitude and so are more sensitive to longer periods; their longest period system is currently HATS-17b at 16.3 d (Brahm et al. 2016).

The mass of WASP-130b is 1.23 ± 0.04 $M_{\rm Jup}$. In keeping with other longer period systems (e.g. Demory & Seager 2011), but in contrast to many hotter Jupiters, the radius is not bloated (0.89 ± 0.03 $R_{\rm Jup}$). WASP-130b is thus similar to HATS-17b (1.34 $M_{\rm Jup}$ and 0.78 $R_{\rm Jup}$; Brahm et al. 2016), though not quite as compact. Brahm et al. suggest that HATS-17b has a massive metallic core, which they link to the raised metallicity of [Fe/H] = +0.3, which is again similar to that of WASP-130 ([Fe/H] = +0.25).

6 WASP-131

WASP-131 is a $V = 10.1$, G0 star with a metallicity of [Fe/H] = −0.18 ± 0.08. The transit log g_* of 4.09 ± 0.03 is consistent with the spectroscopic log g_* of 3.9 ± 0.1. The radius is inflated (1.53 $R_\odot$ for 1.06 $M_\odot$) and the evolutionary comparison (Fig. 15) suggests an age of 4.5–10 Gyr (consistent with the poorly constrained lithium estimate of between 1 and 8 Gyr).

The planet, WASP-131b, has an orbital period of 5.3 d. It is a Saturn-mass but bloated planet (0.27 $M_{\rm Jup}$ and 1.22 $R_{\rm Jup}$). The low density of the planet (0.15 ± 0.02 $\rho_{\rm J}$) and the consequent large scaleheight of the atmosphere, coupled with the host-star magnitude of $V = 10.1$, should make WASP-131b a good candidate for atmospheric characterization.

Low-density, Saturn-mass planets akin to WASP-131b have been seen before. The most similar include WASP-21b (0.28 $M_{\rm Jup}$; 1.2 $R_{\rm Jup}$ and $P = 4.3$ d; Bouchy et al. 2010), WASP-39b (0.28 $M_{\rm Jup}$; 1.3 $R_{\rm Jup}$ and $P = 4.1$ d; Faedi et al. 2011), Kepler-427b (0.29 $M_{\rm Jup}$; 1.2 $R_{\rm Jup}$ and $P = 10.3$ d; Hébrard et al. 2014) and HAT-P-51b (0.30 $M_{\rm Jup}$; 1.3 $R_{\rm Jup}$ and $P = 4.2$ d; Hartman et al. 2015b).

7 WASP-132

WASP-132 is a $V = 12.4$, K4 star with a metallicity of [Fe/H] = +0.22 ± 0.13. The transit log g_* of 4.61 ± 0.02 is consistent with

Table 3. System parameters for WASP-131.

1SWASP J140046.44–303500.8	
2MASS 14004645–3035008	
RA = $14^h00^m46.45^s$, Dec. = $-30°35'00.8''$ (J2000)	
V mag = 10.1	
Rotational modulation < 0.5 mmag (95 per cent)	
pm (RA) 11.4 ± 1.9 (Dec.) –6.5 ± 1.0 mas yr^{-1}	
Stellar parameters from spectroscopic analysis	
Spectral type	G0
$T_{\rm eff}$ (K)	5950 ± 100
log g	3.9 ± 0.1
$v \sin i$ (km s^{-1})	3.0 ± 0.9
[Fe/H]	–0.18 ± 0.08
log A(Li)	2.60 ± 0.08
Age (Lithium) (Gyr)	1 ∼ 8
Distance (pc)	250 ± 50
Parameters from MCMC analysis	
P (d)	5.322023 ± 0.000005
$T_{\rm c}$ (HJD) (UTC)	2456919.8236 ± 0.0004
T_{14} (d)	0.1596 ± 0.0014
$T_{12} = T_{34}$ (d)	0.0243 ± 0.0016
$\Delta F = R_{\rm P}^2/R_*^2$	0.00665 ± 0.00012
b	0.73 ± 0.02
i (°)	85.0 ± 0.3
K_1 (km s^{-1})	0.0305 ± 0.0017
γ (km s^{-1})	–19.6636 ± 0.0015
e	0 (adopted) (<0.10 at 2σ)
$M_\star$ ($M_\odot$)	1.06 ± 0.06
$R_\star$ ($R_\odot$)	1.53 ± 0.05
log g_* (cgs)	4.089 ± 0.026
$\rho_\star$ ($\rho_\odot$)	0.292 ± 0.026
$T_{\rm eff}$ (K)	6030 ± 90
$M_{\rm P}$ ($M_{\rm Jup}$)	0.27 ± 0.02
$R_{\rm P}$ ($R_{\rm Jup}$)	1.22 ± 0.05
log $g_{\rm P}$ (cgs)	2.62 ± 0.04
$\rho_{\rm P}$ ($\rho_{\rm J}$)	0.15 ± 0.02
a (au)	0.0607 ± 0.0009
$T_{\rm P,\,A=0}$ (K)	1460 ± 30

Errors are 1σ; Limb-darkening coefficients were:
r band: a1 = 0.601, a2 = −0.085, a3 = 0.517, a4 = −0.300
I band: a1 = 0.676, a2 = −0.353, a3 = 0.685, a4 = −0.347
z band: a1 = 0.573, a2 = −0.142, a3 = 0.410, a4 = −0.241.

Table 4. System parameters for WASP-132.

1SWASP J143026.22–460933.0	
2MASS 14302619–4609330	
RA = $14^h30^m26.19^s$, Dec. = $-46°09'33.0''$ (J2000)	
V mag = 12.4	
Rotational modulation: possible 0.4-mmag at 33-d.	
pm (RA) 14.2 ± 1.3 (Dec.) –73.8 ± 1.3 mas yr^{-1}	
Stellar parameters from spectroscopic analysis	
Spectral type	K4
$T_{\rm eff}$ (K)	4750 ± 100
log g	4.6 ± 0.1
$v \sin i$ (km s^{-1})	0.9 ± 0.8
[Fe/H]	+0.22 ± 0.13
log A(Li)	<−0.3
Age (Lithium) (Gyr)	$\gtrsim$0.5
Distance (pc)	120 ± 20
Parameters from MCMC analysis	
P (d)	7.133521 ± 0.000009
$T_{\rm c}$ (HJD) (UTC)	2456698.2076 ± 0.0004
T_{14} (d)	0.1284 ± 0.0009
$T_{12} = T_{34}$ (d)	0.0141 ± 0.0008
$\Delta F = R_{\rm P}^2/R_*^2$	0.0146 ± 0.0003
b	0.14 ± 0.12
i (°)	89.6 ± 0.3
K_1 (km s^{-1})	0.051 ± 0.003
γ (km s^{-1})	31.067 ± 0.003
e	0 (adopted) (<0.10 at 2σ)
$M_\star$ ($M_\odot$)	0.80 ± 0.04
$R_\star$ ($R_\odot$)	0.74 ± 0.02
log g_* (cgs)	4.61 ± 0.02
$\rho_\star$ ($\rho_\odot$)	$2.00^{+0.07}_{-0.14}$
$T_{\rm eff}$ (K)	4775 ± 100
$M_{\rm P}$ ($M_{\rm Jup}$)	0.41 ± 0.03
$R_{\rm P}$ ($R_{\rm Jup}$)	0.87 ± 0.03
log $g_{\rm P}$ (cgs)	3.10 ± 0.04
$\rho_{\rm P}$ ($\rho_{\rm J}$)	0.63 ± 0.06
a (au)	0.067 ± 0.001
$T_{\rm P,\,A=0}$ (K)	763 ± 16

Errors are 1σ; Limb-darkening coefficients were:
z band: a1 = 0.742, a2 = −0.751, a3 = 1.200, a4 = −0.498.

the spectroscopic log g_* of 4.6 ± 0.1. The evolutionary comparison (Fig. 15) gives an age of >0.9 Gyr.

The radial velocities show excess scatter, which may be due to magnetic activity. There is also a suggestion in Fig. 5 of a possible correlation of the bisector with orbital phase. This is partly due to a possible longer term trend to both lower radial velocities and bisectors over the span of the observations. The radial velocities decrease by 60 m s^{-1} over time, though this is unreliable owing to the CORALIE upgrade midway through the data set. If we analyse the data before and after the upgrade separately we find no significant correlation between the bisector and the radial-velocity value.

A possible rotational modulation with a period of 33 ± 3 d, and an amplitude of 0.4 mmag, is seen in three out of five seasons of WASP data (Fig. 6), while a possible modulation at half this period is seen in a fourth data set. This is close to the limit detectable with WASP data (for the other stars we are quoting upper limits in the range 0.5–1.5 mmag), and so is not fully reliable.

A rotational period of 33 ± 3 d would indicate a gyrochronological age of 2.2 ± 0.3 Gyr (Barnes 2007), which is consistent with the above evolutionary estimate. The period would also imply an equatorial velocity of 1.1 ± 0.2 km s^{-1}, which is consistent with the observed (but poorly constrained) $v \sin i$ value of 0.9 ± 0.8 km s^{-1}.

The planet, WASP-132b, has a low-mass and a modest radius compared to many hot Jupiters (0.41 $M_{\rm Jup}$ and 0.87 $R_{\rm Jup}$). With an orbital period of 7.1 d around a K4 star it is among the least irradiated of the WASP planets. The equilibrium temperature is estimated at only 763 ± 16 K. Of WASP systems, only WASP-59b (Hébrard et al. 2013), in a 7.9-d orbit around a K5V, has a lower temperature of 670 ± 35 K. HATS-6b (Hartman et al. 2015a), in a 3.3-d orbit around an M1V star, is also cooler (713 ± 5 K), but all other cooler gas giants have orbital periods of greater than 10 d.

8 WASP-139

WASP-139 is a V = 12.4, K0 star with a metallicity of [Fe/H] = +0.20 ± 0.09. The transit log g_* of 4.59 ± 0.06 is consistent with the spectroscopic log g_* of 4.5 ± 0.1. The gyrochonological age constraint and the lack of lithium imply a relatively young star of ∼0.5 Gyr.

The stellar density resulting from the transit analysis ($1.8 \pm 0.2\ \rho_\odot$; 0.92 $M_\odot$ and 0.80 $R_\odot$) puts the star below the main sequence and is only marginally consistent with the evolutionary models of Maxted et al. (2015a). The same has been found for HAT-P-11 (Bakos et al. 2010) and possibly also for WASP-89 (Hellier et al. 2015). For a discussion of this see Maxted, Serenelli & Southworth (2015b), who suggested that such stars might be helium-rich.

The planet, WASP-139b, has a mass of only 0.12 ± 0.02 M_{Jup}, making it the lowest mass WASP discovery yet. With a radius of 0.80 R_{Jup}, and thus a low density of $0.23 \pm 0.04\ \rho_{Jup}$, the large scaleheight makes WASP-139b a good target for atmospheric characterization.

Owing to the small planet mass, and thus the low reflex velocity, we obtained HARPS data in order to better parametrize the system. This included observations of the Rossiter–McLaughlin effect through transit (Fig. 8). If the orbit were aligned, and taking values for the $v \sin i$ and impact parameter from Table 5, we would expect an R–M effect of order 30 m s^{-1} (e.g. Gaudi & Winn 2007). The HARPS data indicate a much lower value, though owing to the relatively large errors the fit is effectively unconstrained and thus we do not report parameters such as the alignment angle.

WASP-139b is most similar to two recent discoveries by the HATSouth project, HATS-7b (Bakos et al. 2015) and HATS-8b (Bayliss et al. 2015). HATS-7b is a 0.12 M_{Jup} planet with a radius of 0.56 R_{Jup} in a 3.2-d orbit. The host stars are also similar (HATS-7 is a $V = 13.3$, K dwarf, $T_{eff} = 4985$, [Fe/H] $= +0.25$; HATS-8 is a $V = 14.0$, G dwarf, $T_{eff} = 5680$, [Fe/H] $= +0.21$; whereas WASP-139 is a $V = 12.4$, K0 dwarf, $T_{eff} = 5300$, [Fe/H] $= +0.20$). The HATS project has called such systems 'super-Neptunes', and, as now the brightest example, the WASP-139 system will be important for studying such objects.

Table 5. System parameters for WASP-139.

1SWASP J031814.91–411807.4	
2MASS 03181493–4118077	
RA = $03^h18^m14.93^s$, Dec. = $-41°18'07.7''$ (J2000)	
V mag = 12.4	
Rotational modulation < 1 mmag (95 per cent)	
pm (RA) –16.7 ± 1.3 (Dec.) 23.6 ± 3.3 mas yr^{-1}	
Stellar parameters from spectroscopic analysis	
Spectral type	K0
T_{eff} (K)	5300 ± 100
log g	4.5 ± 0.1
$v \sin i$ (km s^{-1})	4.2 ± 1.1
[Fe/H]	$+0.20 \pm 0.09$
log A(Li)	<0.5
Age (Lithium) (Gyr)	$\gtrsim$0.5
Age (Gyro) (Gyr)	$< 0.5^{+0.4}_{-0.3}$
Distance (pc)	230 ± 40
Parameters from MCMC analysis	
P (d)	5.924262 ± 0.000004
T_c (HJD) (UTC)	2457196.7933 ± 0.0003
T_{14} (d)	0.118 ± 0.001
$T_{12} = T_{34}$ (d)	0.012 ± 0.002
$\Delta F = R_P^2/R_*^2$	0.0107 ± 0.0003
b	0.33 ± 0.14
i (°)	88.9 ± 0.5
K_1 (km s^{-1})	0.0140 ± 0.0014
γ (km s^{-1})	-12.996 ± 0.001
e	0 (adopted) (<0.28 at 2σ)
$M_\star$ ($M_\odot$)	0.92 ± 0.10
$R_\star$ ($R_\odot$)	0.80 ± 0.04
log g_* (cgs)	4.59 ± 0.06
$\rho_\star$ ($\rho_\odot$)	1.8 ± 0.2
T_{eff} (K)	5310 ± 90
M_P (M_{Jup})	0.117 ± 0.017
R_P (R_{Jup})	0.80 ± 0.05
log g_P (cgs)	2.62 ± 0.06
ρ_P (ρ_J)	0.23 ± 0.04
a (au)	0.062 ± 0.002
$T_{P,\,A=0}$ (K)	910 ± 30

Errors are 1σ; Limb-darkening coefficients were:
r band: a1 = 0.712, a2 = −0.642, a3 = 1.321, a4 = −0.598
z band: a1 = 0.721, a2 = −0.671, a3 = 1.104, a4 = −0.494.

Table 6. System parameters for WASP-140.

1SWASP J040132.53–202703.9	
2MASS 04013254–2027039	
RA = $04^h01^m32.54^s$, Dec. = $-20°27'03.9''$ (J2000)	
V mag = 11.1	
Rotational modulation: 5–9 mmag at 10.4 ± 0.1 d	
pm (RA) –23.2 ± 1.7 (Dec.) 17.8 ± 1.1 mas yr^{-1}	
Stellar parameters from spectroscopic analysis	
Spectral type	K0
T_{eff} (K)	5300 ± 100
log g	4.2 ± 0.1
$v \sin i$ (km s^{-1})	3.1 ± 0.8
[Fe/H]	$+0.12 \pm 0.10$
log A(Li)	<0.4
Age (Lithium) (Gyr)	$\gtrsim$0.5
Age (Gyro) (Gyr)	$< 1.6^{+1.4}_{-0.9}$
Distance (pc)	180 ± 30
Parameters from MCMC analysis	
P (d)	2.2359835 ± 0.0000008
T_c (HJD)	$2456912.35105 \pm 0.00015$
T_{14} (d)	0.0631 ± 0.0009
$T_{12} = T_{34}$ (d)	(undefined)
$\Delta F = R_P^2/R_*^2$	$0.0205\ ^{+0.002}_{-0.0005}$
b	$0.93\ ^{+0.07}_{-0.03}$
i (°)	$83.3\ ^{+0.5}_{-0.8}$
K_1 (km s^{-1})	0.403 ± 0.003
γ (km s^{-1})	2.125 ± 0.003
$e \cos \omega$	0.0468 ± 0.0035
$e \sin \omega$	-0.003 ± 0.006
e	0.0470 ± 0.0035
ω (°)	-4 ± 8
$\phi_{mid\text{-}occultation}$	0.530 ± 0.002
$M_\star$ ($M_\odot$)	0.90 ± 0.04
$R_\star$ ($R_\odot$)	0.87 ± 0.04
log g_* (cgs)	4.51 ± 0.04
$\rho_\star$ ($\rho_\odot$)	1.38 ± 0.18
T_{eff} (K)	5260 ± 100
M_P (M_{Jup})	2.44 ± 0.07
R_P (R_{Jup})	$1.44\ ^{+0.42}_{-0.18}$
log g_P (cgs)	3.4 ± 0.2
ρ_P (ρ_J)	0.8 ± 0.4
a (au)	0.0323 ± 0.0005
$T_{P,\,A=0}$ (K)	1320 ± 40

Errors are 1σ; Limb-darkening coefficients were:
z band: a1 = 0.725, a2 = −0.684, a3 = 1.121, a4 = −0.496
I band: a1 = 0.786, a2 = −0.811, a3 = 1.320, a4 = −0.573

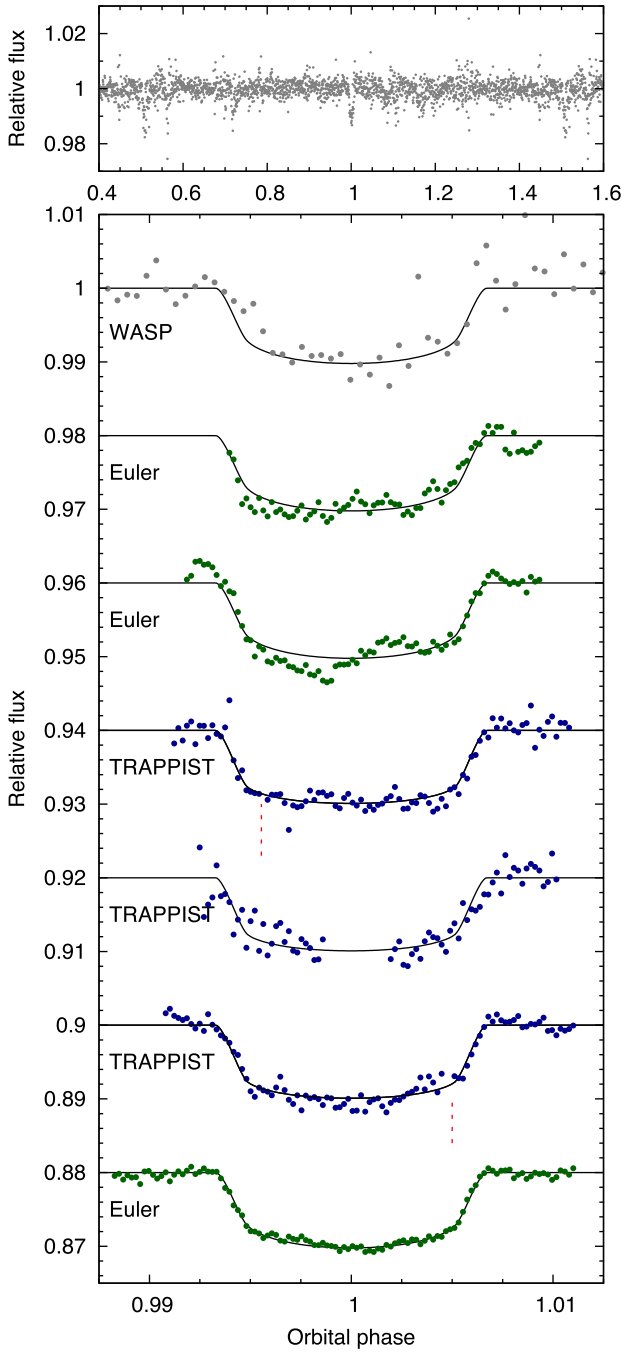

Figure 1. WASP-130b discovery photometry: top: the WASP data folded on the transit period. Second panel: the binned WASP data with (offset) the follow-up transit light curves (ordered from the top as in Table 1) together with the fitted MCMC model. Red dashed lines indicate times when the TRAPPIST photometer was flipped across the meridian. The second EulerCAM light curve had poor observing conditions and shows excess red noise, which was accounted for by inflating the errors in the MCMC process.

9 WASP-140

WASP-140A is a $V = 11.1$, K0 star with a metallicity of [Fe/H] $= +0.12 \pm 0.10$. The transit log g_* of 4.51 ± 0.04 is higher than the spectroscopic log g_* of 4.2 ± 0.1. In such cases we regard the transit value as the more reliable, given the systematic uncertainties in log g_* estimates in such spectra (e.g. Brewer et al. 2015 report discrepancies as big as 0.3 dex).

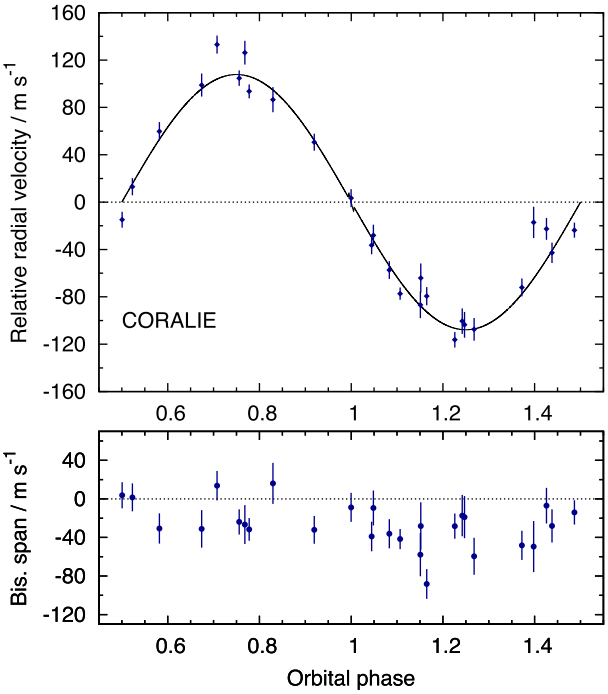

Figure 2. WASP-130b radial velocities and fitted model (top) along with (bottom) the bisector spans; the absence of any correlation with radial velocity is a check against transit mimics.

A second star, WASP-140B, is fainter by 2.01 ± 0.02 mag and is 7.24 ± 0.01 arcsec from WASP-140 at a position angle of 77.4 ± 0.1 deg (values from the EulerCAM observation on 2015 September 01 with an I_c filter). The TRAPPIST and EulerCAM transit photometry used a small aperture that excluded this star. The 2MASS colours of WASP-140B ($J = 11.09 \pm 0.03$; $H = 10.46 \pm 0.02$ and $Ks = 10.27 \pm 0.03$) are consistent with it being physically associated with WASP-140A ($J = 9.61 \pm 0.03$; $H = 9.24 \pm 0.02$ and $Ks = 9.17 \pm 0.03$), and so it is possible that the two stars form a binary. There are no proper motion values listed for WASP-140B in UCAC4.

The WASP data on WASP-140 show a clear rotational modulation with a period of 10.4 ± 0.1 d and an amplitude varying between 5 and 9 mmag (Fig. 11), implying that it is magnetically active. The WASP aperture includes both stars, so it is not certain which star is the variable, though if it were WASP-140B then the amplitude would have to be six times higher, which is less likely. There is also evidence of a star spot in each of the two lowest transit light curves in Fig. 9, which would imply that WASP-140A is magnetically active.

The 10.4-d rotational period would imply a young gyrochronological age for WASP-140A of 0.42 ± 0.06 Gyr (Barnes 2007). This is inconsistent with the evolutionary comparison (Fig. 15), which suggests a likeliest age of 8 Gyr with a lower bound of 1.7 Gyr. This inconsistency suggests that WASP-140A has been spun up by the presence of the massive, closely orbiting planet (see the discussion in Brown 2014).

The rotational period equates to an equatorial velocity of 6.3 ± 0.9 km s^{-1}. Comparing this to the observed $v \sin i$ value of 3.1 ± 0.8 km s^{-1} suggests a misaligned system, with the star's spin axis at an inclination of $30^\circ \pm 15^\circ$.

The planet WASP-140Ab has a mass of 2.4 M_{Jup} and is in a 2.2-d orbit. The transit is grazing, with an impact parameter of

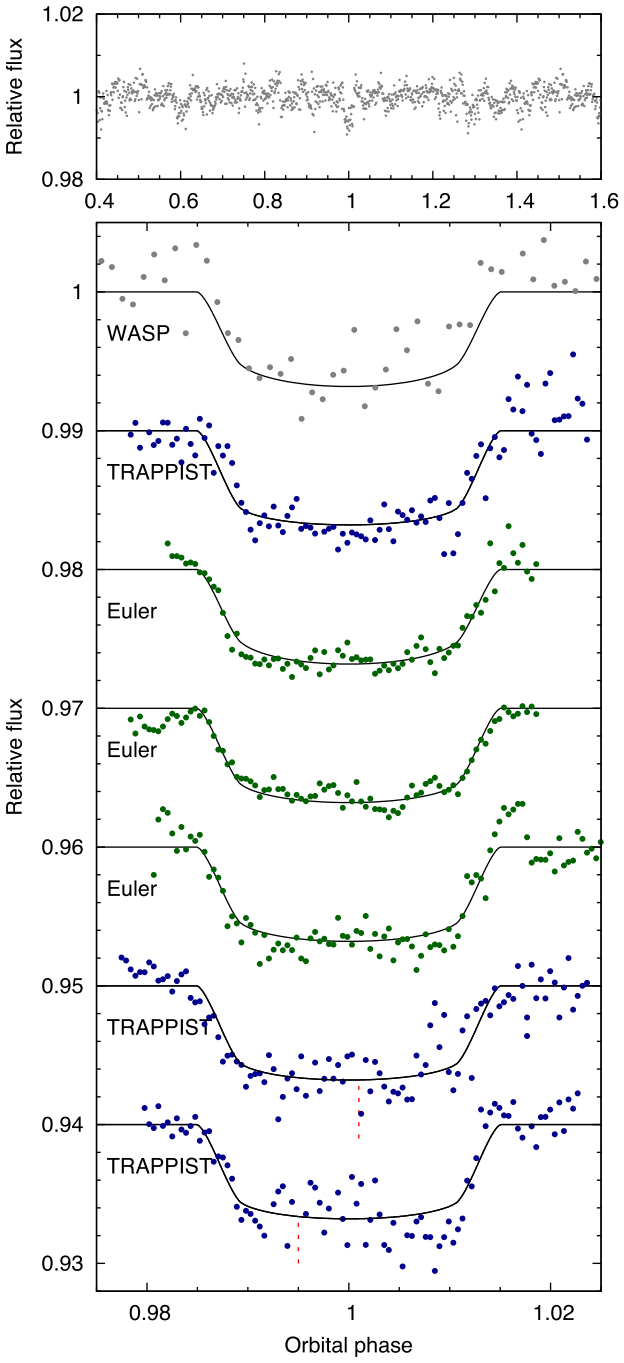

Figure 3. WASP-131b discovery photometry, as for Fig. 1.

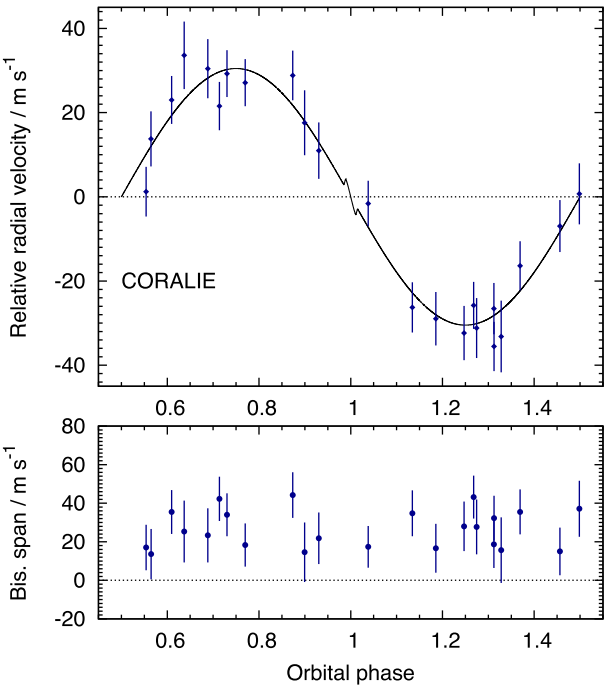

Figure 4. WASP-131b radial velocities and bisector spans, as for Fig. 2.

0.93 $^{+0.07}_{-0.03}$. Other WASP planets that are grazing are WASP-67b (Hellier et al. 2012; Mancini et al. 2014) and WASP-34b (Smalley et al. 2011). Since it is possible that not all of the planet is transiting the star its radius is ill-constrained at 1.44 $^{+0.42}_{-0.18}$ R_{Jup}.

9.1 WASP-140Ab's eccentric orbit

The orbit of WASP-140Ab is eccentric with $e = 0.0470 \pm 0.0035$. A Lucy–Sweeney test shows this to be significantly non-zero with >99.9 per cent confidence. Being significantly eccentric at an orbital period as short as 2.2 d is unusual in a hot Jupiter. For comparison, WASP-14b (Joshi et al. 2009) also has an eccentric 2.2-d orbital period, but is a much more massive planet at 7.7 M_{Jup}. WASP-89b (Hellier et al. 2015) has an eccentric 3.4-d orbit and is also more massive at 5.9 M_{Jup}.

The circularization time-scale for a hot Jupiter can be estimated from [Adams & Laughlin 2006, equation (3)]:

$$\tau_{\rm cir} \approx 1.6\,{\rm Gyr} \times \left(\frac{Q_{\rm P}}{10^6}\right) \times \left(\frac{M_{\rm P}}{M_{\rm Jup}}\right) \times \left(\frac{M_*}{M_\odot}\right)^{-3/2} \times \left(\frac{R_{\rm P}}{R_{\rm Jup}}\right)^{-5} \times \left(\frac{a}{0.05{\rm au}}\right)^{13/2}$$

Using a value of the quality factor, Q_P, of 10^5 (e.g. Socrates, Katz & Dong 2012), and the parameters of Table 6, gives a circularization time-scale of ∼5 Myr. Note, however, the strong dependence on R_P, which is poorly constrained in WASP-140Ab owing to the grazing transit. Pushing Q_P up to 10^6, and taking the parameters at their 1σ boundaries to lengthen the time-scale allows values of ∼100 Myr. This is still short compared to the likely age of the host star, and suggests that WASP-140b has only relatively recently arrived in its current orbit.

Comparing to other hot-Jupiters, using the above equation and parameters tabulated in TEPCat (Southworth 2011), we find that WASP-140Ab has the shortest circularization time-scale of all hot Jupiters that are in clearly eccentric orbits (where we adopt a 3σ threshold). Using the best-fitting parameters of Table 6 for WASP-140Ab, and adopting $Q_P = 10^5$, gives $\log(\tau_{\rm cir}) = 6.6$.

A time-scale of $\log(\tau_{\rm cir}) = 6.1$ is obtained for WASP-18b (Hellier et al. 2009), which has been reported as having a small but significant eccentricity of $e = 0.008 \pm 0.001$ (Triaud et al. 2010). However, this apparent eccentricity might instead be an effect of the tidal bulge on WASP-18, which is the biggest of any known hot-Jupiter system (see Arras et al. 2012).

The next shortest time-scale is $\log(\tau_{\rm cir}) = 6.8$ for HAT-P-13b (Bakos et al. 2009). From *Spitzer* observations of the planetary occulation, Buhler et al. (2016) report a significant eccentricity of

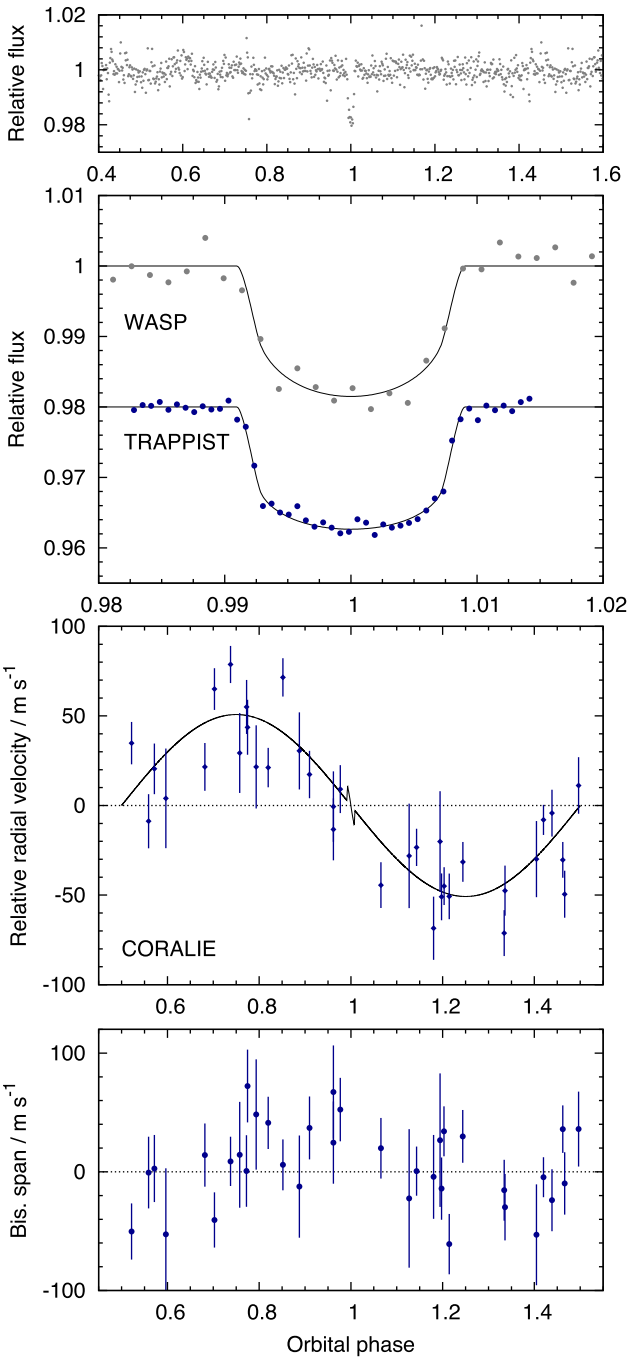

Figure 5. WASP-132b discovery data, as for Figs 1 and 2.

$e = 0.007 \pm 0.001$. In this system, however, the eccentricity of the hot Jupiter HAT-P-13b is likely being maintained by the perturbative effect of HAT-P-13c, a 14 M_{Jup} outer planet in a highly eccentric ($e = 0.66$) 446-d orbit (Winn et al. 2010).

The smallest time-scale for any other hot Jupiter that is indisputably eccentric is likely that for WASP-14b at $\log(\tau_{cir}) = 7.6$. This is an order of magnitude longer than that for WASP-140Ab, which implies that WASP-140Ab is unusual. Tidal heating has long been proposed as a possible cause of the inflated radii of many hot Jupiters (e.g. Socrates 2013 and references therein), and may help to explain the fact that WASP-140Ab has a bloated radius despite being relatively massive. It will be worth obtaining better transit photometry of WASP-140, in order to better constrain the parameters, and also worth looking for an outer planet that might be maintaining the eccentricity.

It is also worth noting that short-period, massive and eccentric planets are rare around K stars. WASP-89b is the previously known example, a 6 M_{Jup} planet in a 3.36-d orbit with an eccentricity of 0.192 ± 0.009 around a K3 star (Hellier et al. 2015). The magnetic activity of both stars, WASP-89 and WASP-140A, might be related to the presence of the eccentric, short-period planet (e.g. Poppenhaeger & Wolk 2014).

10 WASP-141

WASP-141 is a $V = 12.4$, F9 star with a metallicity of [Fe/H] $= +0.29 \pm 0.09$. The transit $\log g_*$ of 4.26 ± 0.06 is consistent with the spectroscopic value of 4.20 ± 0.15. The evolutionary comparison (Fig. 15) gives an age estimate of 1.5–5.6 Gyr. This is compatible with the gyrochronological estimate of $< 4.0^{+4.6}_{-2.4}$ Gyr and marginally consistent with the lithium age of $\gtrsim 5$ Gyr.

Table 7. System parameters for WASP-141.

1SWASP J044717.84–170654.6	
2MASS 04471785–1706545	
RA = $04^h47^m17.85^s$, Dec. = $-17°06'54.5''$ (J2000)	
V mag = 12.4	
Rotational modulation < 1.5 mmag (95 per cent)	
pm (RA) 4.2 ± 0.9 (Dec.) -3.1 ± 2.6 mas yr^{-1}	
Stellar parameters from spectroscopic analysis	
Spectral type	F9
T_{eff} (K)	6050 ± 120
$\log g$	4.20 ± 0.15
$v \sin i$ (km s^{-1})	3.9 ± 0.8
[Fe/H]	$+0.29 \pm 0.09$
log A(Li)	1.75 ± 0.12
Age (Lithium) (Gyr)	$\gtrsim 5$
Age (Gyro) (Gyr)	$< 4.0^{+4.6}_{-2.4}$
Distance (pc)	570 ± 150
Parameters from MCMC analysis	
P (d)	3.310651 ± 0.000005
T_c (HJD) (UTC)	2457019.5953 ± 0.0003
T_{14} (d)	0.150 ± 0.001
$T_{12} = T_{34}$ (d)	0.014 ± 0.001
$\Delta F = R_P^2/R_*^2$	0.0083 ± 0.0002
b	0.31 ± 0.12
i (°)	87.6 ± 1.3
K_1 (km s^{-1})	0.315 ± 0.015
γ (km s^{-1})	33.828 ± 0.009
e	0 (adopted) (<0.06 at 2σ)
$M_\star$ ($M_\odot$)	1.25 ± 0.06
$R_\star$ ($R_\odot$)	1.37 ± 0.07
$\log g_*$ (cgs)	4.26 ± 0.04
$\rho_\star$ ($\rho_\odot$)	0.49 ± 0.07
T_{eff} (K)	5900 ± 120
M_P (M_{Jup})	2.69 ± 0.15
R_P (R_{Jup})	1.21 ± 0.08
$\log g_P$ (cgs)	3.62 ± 0.05
ρ_P (ρ_J)	1.49 ± 0.25
a (au)	0.0469 ± 0.0007
$T_{P,A=0}$ (K)	1540 ± 50
Errors are 1σ; Limb-darkening coefficients were: z band: a1 = 0.616, a2 = −0.305, a3 = 0.635, a4 = −0.331.	

The planet, WASP-141b is a 2.7 M_{Jup}, 1.2 R_{Jup} planet in a 3.3-d orbit. WASP-141 appears to be a typical hot-Jupiter system.

11 WASP-142

WASP-142A is a $V = 12.3$, F8 star with a metallicity of [Fe/H] $= +0.26 \pm 0.12$. The transit log g_* of 4.13 ± 0.04 is consistent with the spectroscopic value of 4.0 ± 0.2. The evolutionary comparison (Fig. 15) gives an age estimate of 2.2–7.0 Gyr. The lithium age is marginally inconsistent at $\lesssim$2 Gyr.

A second star, WASP-142B, is fainter by 1.86 ± 0.01 mag and at 5.11 ± 0.01 arcsec from WASP-142 at a position angle of -45.7 ± 0.1 deg (values from an EulerCAM observation on 2014 December 13 with an I_c filter). The 2014 December EulerCAM transit photometry used an aperture including both stars, and we corrected the light curve for the dilution in the analysis. The other EulerCAM transit and the two TRAPPIST transits used a smaller photometric aperture excluding the second star.

Table 8. System parameters for WASP-142.

1SWASP J092201.43–235645.8	
2MASS 09220153–2356462	
RA $= 09^h22^m01.53^s$, Dec. $= -23°56'46.2''$ (J2000)	
V mag $= 12.3$	
Rotational modulation < 1.5 mmag (95 per cent)	
pm (RA) -3.1 ± 3.5 (Dec.) 3.7 ± 3.1 mas yr^{-1}	
Stellar parameters from spectroscopic analysis	
Spectral type	F8
$T_{\rm eff}$ (K)	6060 ± 150
log g	4.0 ± 0.2
$v \sin i$ (km s^{-1})	3.1 ± 1.4
[Fe/H]	$+0.26 \pm 0.12$
log A(Li)	3.10 ± 0.09
Age (Lithium) (Gyr)	$\lesssim$2
Distance (pc)	840 ± 310
Parameters from MCMC analysis	
P (d)	2.052868 ± 0.000002
T_c (HJD)	2457007.7779 ± 0.0004
T_{14} (d)	0.1117 ± 0.0016
$T_{12} = T_{34}$ (d)	0.022 ± 0.002
$\Delta F = R_P^2/R_*^2$	0.00916 ± 0.00026
b	0.77 ± 0.02
i (°)	80.2 ± 0.6
K_1 (km s^{-1})	0.109 ± 0.010
γ (km s^{-1})	47.126 ± 0.010
e	0 (adopted) ($<$0.27 at 2σ)
$M_\star$ ($M_\odot$)	1.33 ± 0.08
$R_\star$ ($R_\odot$)	1.64 ± 0.08
log g_* (cgs)	4.13 ± 0.04
$\rho_\star$ ($\rho_\odot$)	0.30 ± 0.04
$T_{\rm eff}$ (K)	6010 ± 140
M_P (M_{Jup})	0.84 ± 0.09
R_P (R_{Jup})	1.53 ± 0.08
log g_P (cgs)	2.91 ± 0.06
ρ_P (ρ_J)	0.23 ± 0.05
a (au)	0.0347 ± 0.0007
$T_{P,\,A=0}$ (K)	2000 ± 60

Errors are 1σ; Limb-darkening coefficients were:
z band: a1 $= 0.570$, a2 $= -0.130$, a3 $= 0.391$, a4 $= -0.233$
I band: a1 $= 0.673$, a2 $= -0.340$, a3 $= 0.666$, a4 $= -0.340$.

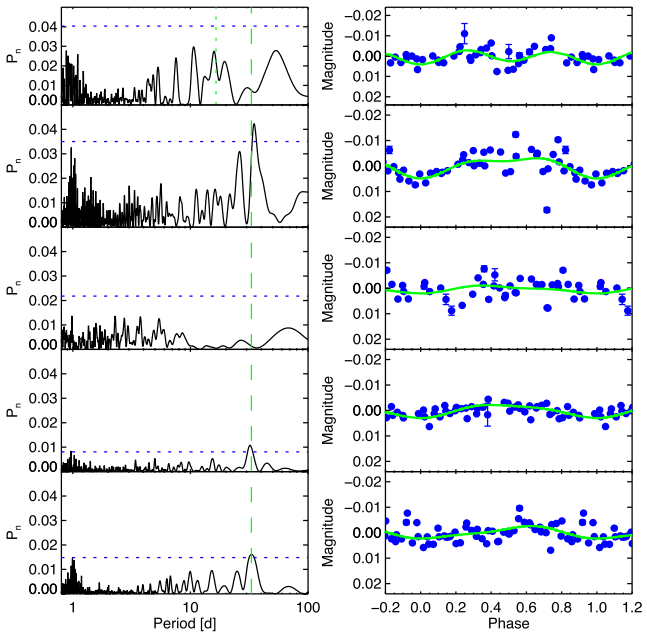

Figure 6. Possible rotational modulation in the WASP data for WASP-132. The left-hand panels show peridograms for each season of data (2006, 2007, 2008, 2011 and 2012 from the top down). The 33-d period is marked in green, as is half this period in the uppermost panel. The blue dotted line is a false-alarm probability of 0.001. The right-hand panels show the data for each season folded on the 33.4-d period; the green line is a harmonic-series fit to the data.

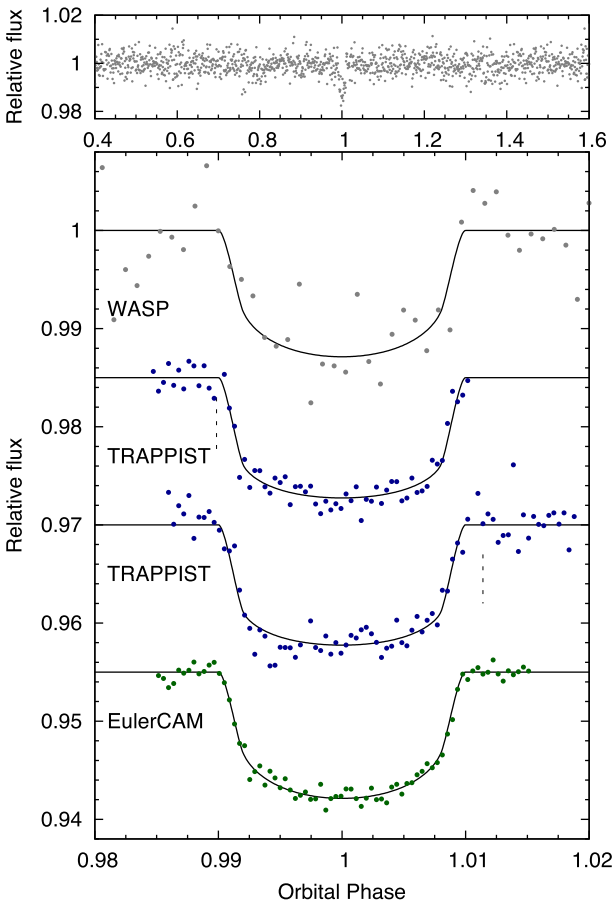

Figure 7. WASP-139b discovery photometry, as for Fig. 1.

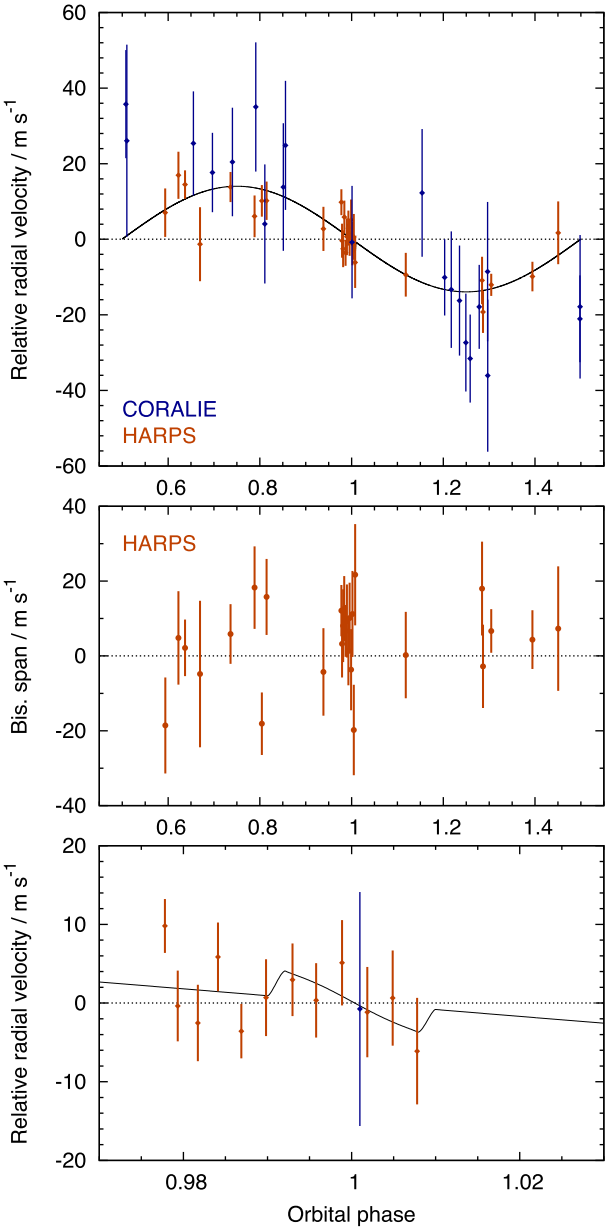

Figure 8. WASP-139b radial velocities and bisector spans, as for Fig. 2. We have not plotted three RV points with very large errors. We also show only the HARPS bisectors, which have smaller errors. The lowest panel is a larger scale view of the transit and the R–M effect.

The 2MASS colours of WASP-142B (J = 13.42 ± 0.04; H = 13.03 ± 0.04 and Ks = 12.94 ± 0.03) are consistent with it being physically associated with WASP-142A (J = 11.73 ± 0.03; H = 11.48 ± 0.03 and Ks = 11.44 ± 0.03). UCAC4, however, reports a very different proper motion for WASP-142B (pmRA = −99.1 ± 2.1 and pmDec. = 98.3 ± 2.2 mas yr^{-1}) than for WASP-142A (pmRA = −3.1 ± 3.5 and pmDec. = 3.7 ± 3.1 mas yr^{-1}), which, if reliable, would rule out a physical association.

WASP-142Ab is a bloated planet of sub-Jupiter mass (1.53 R_{Jup} and 0.84 M_{Jup}) in a 2.1-d orbit. Again, WASP-142 is a fairly typical hot-Jupiter system.

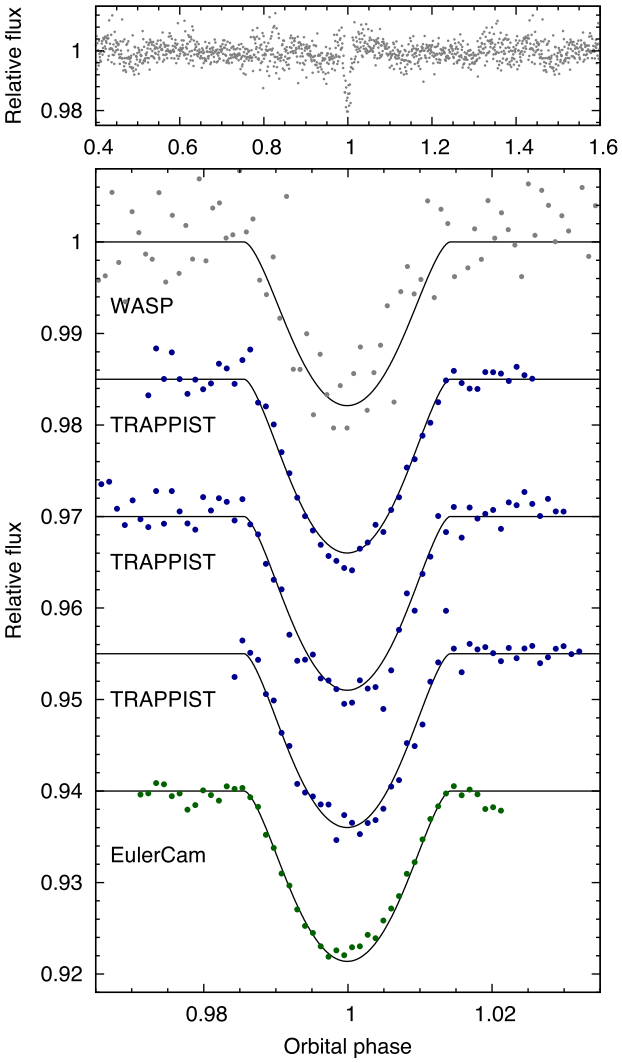

Figure 9. WASP-140b photometry, as for Fig. 1.

12 HOT JUPITER PERIOD DISTRIBUTION

We take the opportunity to revisit the period distribution of gas giants in close orbits. We have thus taken all planets with masses 0.15–12 M_{Jup} listed in TEPCat, and added the unpublished WASP planets as far as WASP-166b, and plot the cumulative period distribution in Fig. 16. This figure contains 321 planets out to 22 d, nearly doubling the 163 planets in the similar analysis in Hellier et al. (2012).

The two 'breaks' suggested by Hellier et al. (2012) at 1.2 and 2.7 d are still present. The systems with periods <1.2 d are rare, despite having a greater range of inclinations that produce a transit, and despite being the easiest to find in transit surveys. They likely have short lifetimes owing to tidal inspiral. Above 2.7 d, the hot-Jupiter 'pileup' continues to a more gradual rollover over the range 4–7 d. Above ∼8 or 9 d the ground-based transit surveys will be less sensitive, and so one should be cautious in interpreting the distribution at longer periods.

Dawson & Murray-Clay (2013) analysed the *Kepler* sample of giant planets and found that the period distribution was strongly dependent on the metallicity of the host star (their fig. 4). They

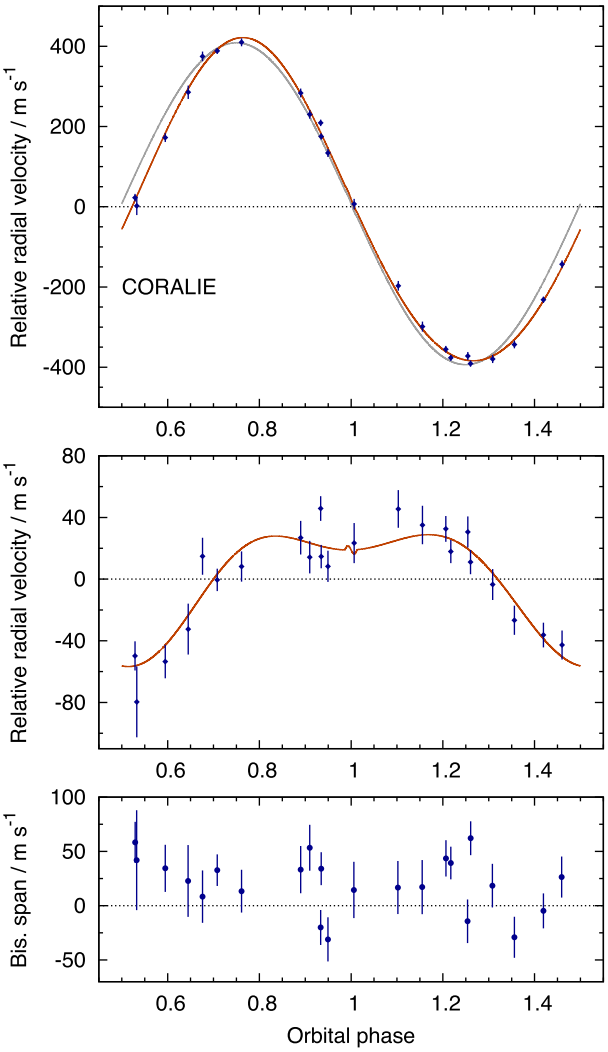

Figure 10. WASP-140b radial velocities, as for Fig. 2. Top: the dark-orange radial velocity curve is the best-fitting eccentric orbit; the grey line is the best circular orbit for comparison. Middle: the RVs after subtracting the circular orbit. Lowest: the bisector spans.

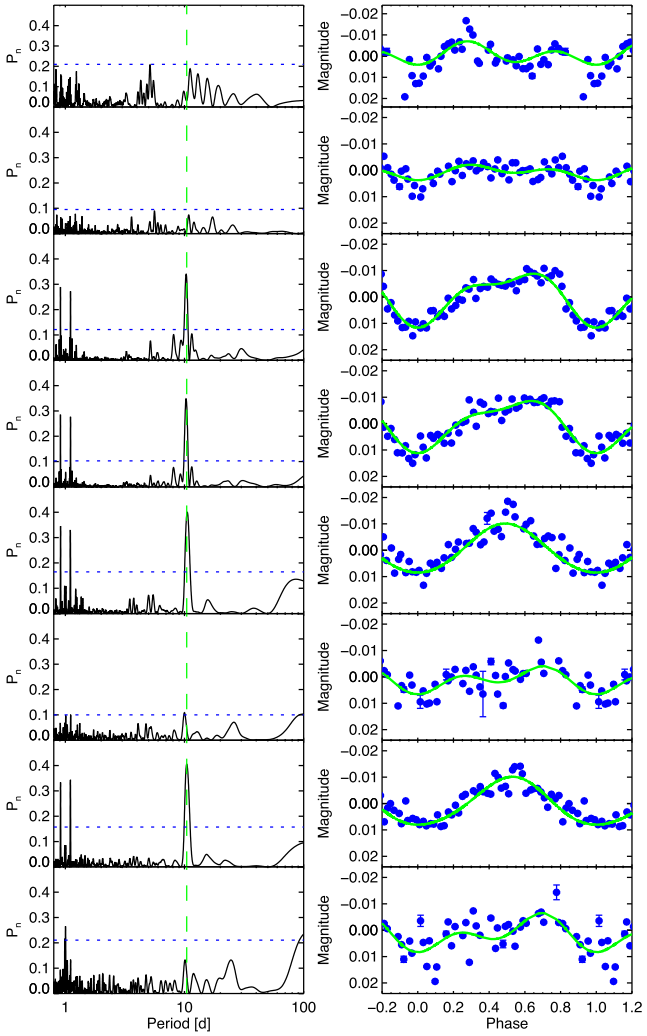

Figure 11. Rotational modulation in the WASP data for WASP-140. The left-hand panels show peridograms for independent data sets (a season of data in a given camera over 2006–2011). The blue dotted line is a false-alarm probability of 0.001. The right-hand panels show the data for each season folded on the 10.4-d period; the green line is a harmonic-series fit to the data.

suggested that the hot-Jupiter bulge is a feature only of metal-rich stars, and that the excess of hot Jupiters relative to longer period giant planets is not present in a sample with [Fe/H] < 0. Note, however, that their analysis depended on the use of KIC metallicities, which come from photometric colours and thus may not be fully reliable (Dong et al. 2014).

Our above sample has very few planets beyond $P > 10$ d and so cannot be used to test the Dawson & Murray-Clay (2013) result itself. We can, however, address the related question of whether the period distribution *within* the hot-Jupiter bulge has a metallicity dependence, as might be the case if the formation of hot Jupiters depends strongly on metallicity. We thus take all the planets in our sample with host-star metallicities listed in TEPCat, plus those in this paper, noting that these metallicities come from spectroscopic analyses of relatively bright host stars.

We then divide the sample into metallicities above and below solar (192 and 79 planets, respectively). The two distributions are compared (after normalizing them) in Fig. 16. A K–S test says that they are not significantly different, with a 40 per cent chance of being drawn from the same distribution. Thus, there does not appear to be a metallicity dependence of the period distribution *within* the hot-Jupiter bulge, though the discovery of more longer period giant planets is needed to test the Dawson & Murray-Clay (2013) result itself.

13 CONCLUSIONS

The ongoing WASP surveys continue to discover novel objects which push the bounds of known exoplanets (e.g. the rapid circularization time-scale of WASP-140b) along with planets transiting bright stars which are good targets for atmospheric characterization (e.g. WASP-131b, with a $V = 10.1$ star). We also present the longest period (WASP-130b), lowest mass (WASP-139b) and second-coolest (WASP-132b) of WASP-discovered planets. We also demonstrate the power of WASP photometry in the possible detection of a 0.4-mmag rotational modulation of the star WASP-132.

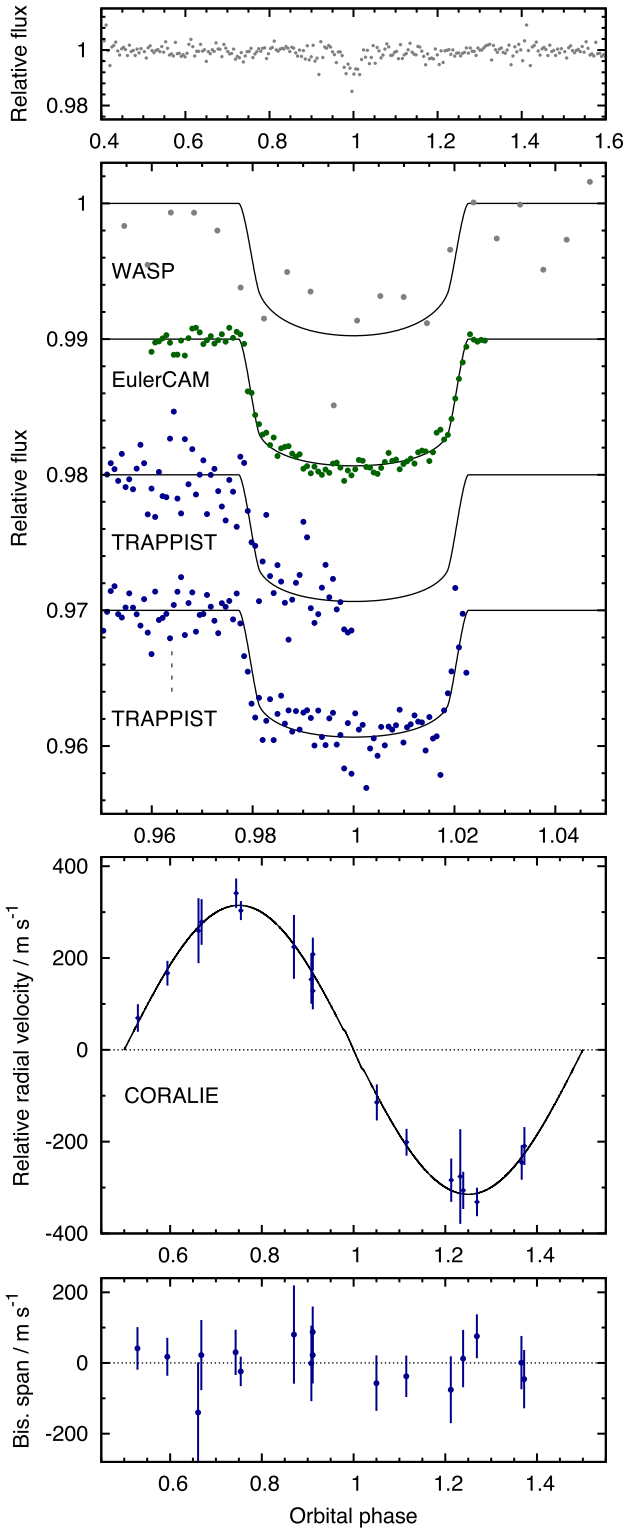

Figure 12. WASP-141b discovery data, as for Figs 1 and 2.

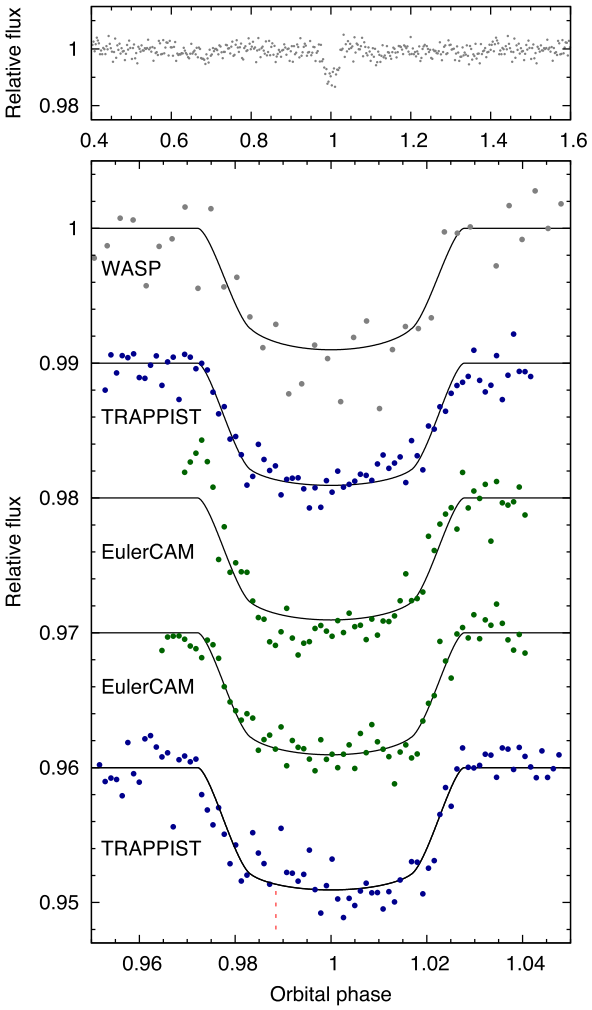

Figure 13. WASP-142b discovery photometry, as for Fig. 1.

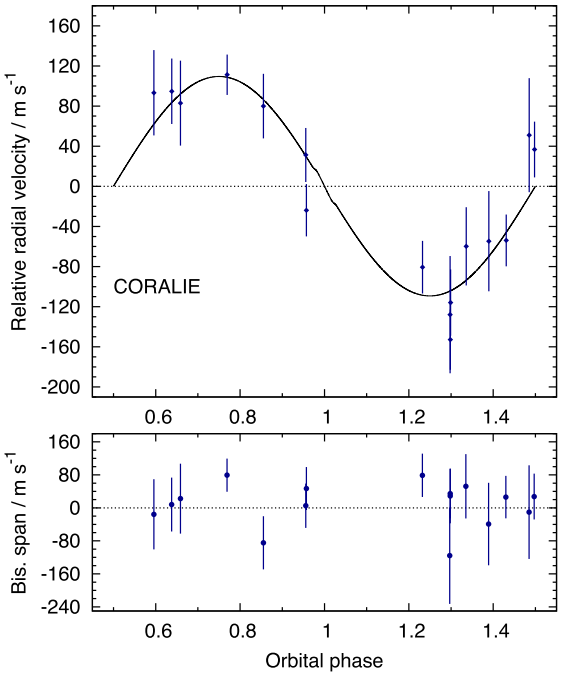

Figure 14. WASP-142b radial velocities and bisector spans, as for Fig. 2.

ACKNOWLEDGEMENTS

WASP-South is hosted by the South African Astronomical Observatory and we are grateful for their ongoing support and assistance. Funding for WASP comes from consortium universities and from the UK's Science and Technology Facilities Council. The Euler

Table 9. Bayesian mass and age estimates for the host stars.

Star	Likeliest age (Gyr)	95 per cent range (Gyr)	Mass ($M_\odot$)
WASP-130	1.4	0.2–7.9	1.03 ± 0.04
WASP-131	7.5	4.5–10.1	1.06 ± 0.06
WASP-132	1.8	>0.9	0.80 ± 0.04
WASP-139	0.0	<9.8	0.92 ± 0.04
WASP-140	8.3	>1.7	0.90 ± 0.04
WASP-141	3.2	1.5–5.6	1.25 ± 0.06
WASP-142	3.6	2.2–7.0	1.32 ± 0.08

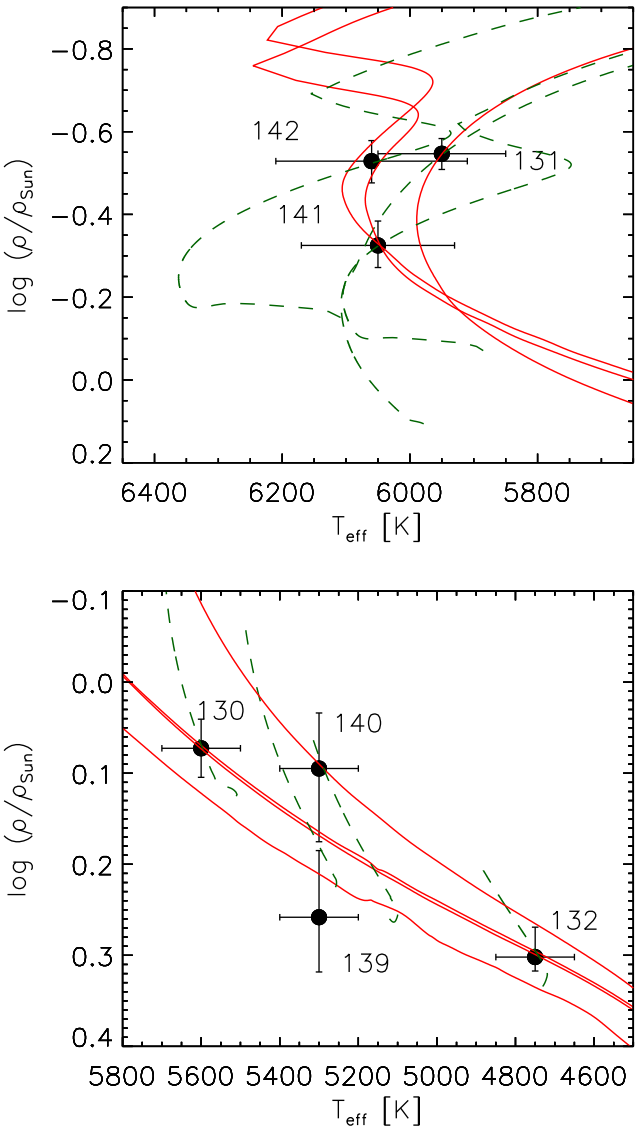

Figure 15. Mean stellar densities versus effective temperatures. Each planet is plotted with the mass track (green-dashed line) and isochrone (red line) for the best-fitting mass and age as listed in Table 9.

Swiss telescope is supported by the Swiss National Science Foundation. TRAPPIST is funded by the Belgian Fund for Scientific Research (Fond National de la Recherche Scientifique, FNRS) under the grant FRFC 2.5.594.09.F, with the participation of the Swiss National Science Foundation (SNF). We acknowledge use of the ESO 3.6 m/HARPS under program 094.C-0090.

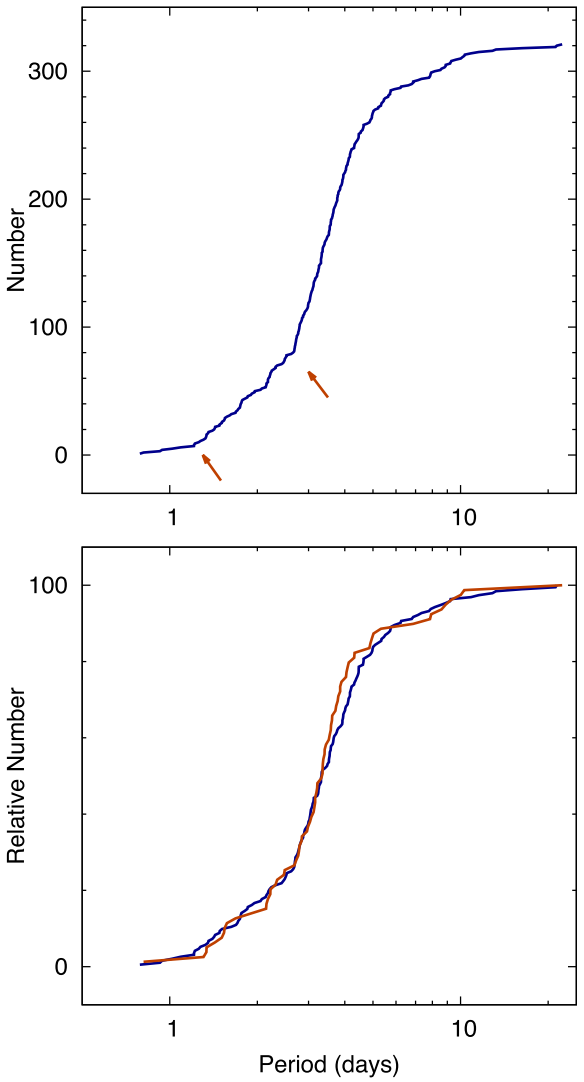

Figure 16. The cumulative period distribution for transiting planets in the range 0.15–12 M_{Jup}. The red arrows mark breaks at 1.2 and 2.7 d suggested by Hellier et al. (2012). The lower panel compares the distributions for planets with host stars of above-solar (blue) and below-solar (red) metallicities.

REFERENCES

Adams F. C., Laughlin G., 2006, ApJ, 649, 1004
Anderson D. R. et al., 2012, MNRAS, 422, 1988
Anderson D. R. et al., 2014, MNRAS, 445, 1114
Arras P., Burkart J., Quataert E., Weinberg N. N., 2012, MNRAS, 422, 1761
Asplund M., Grevesse N., Sauval A. J., Scott P., 2009, ARA&A, 47, 481
Bakos G. Á. et al., 2009, ApJ, 707, 446
Bakos G. Á. et al., 2010, ApJ, 710, 1724
Bakos G. Á. et al., 2015, ApJ, 813, 111
Barnes S. A., 2007, ApJ, 669, 1167
Bayliss D. et al., 2015, AJ, 150, 49
Bouchy F. et al., 2010, A&A, 519, A98
Brahm R. et al., 2016, AJ, 151, 89
Brewer J. M., Fischer D. A., Basu S., Valenti J. A., Piskunov N., 2015, ApJ, 805, 126
Brown D. J. A., 2014, MNRAS, 442, 1844
Buhler P. B., Knutson H. A., Batygin K., Fulton B. J., Fortney J. J., Burrows A., Wong I., 2016, ApJ, 821, 26
Claret A., 2000, A&A, 363, 1081

Collier Cameron A. et al., 2007a, MNRAS, 375, 951
Collier Cameron A. et al., 2007b, MNRAS, 380, 1230
Dawson R. I., Murray-Clay R. A., 2013, ApJ, 767, L24
Demory B.-O., Seager S., 2011, ApJS, 197, 12
Dong S. et al., 2014, ApJ, 789, L3
Doyle A. P. et al., 2013, MNRAS, 428, 3164
Doyle A. P., Davies G. R., Smalley B., Chaplin W. J., Elsworth Y., 2014, MNRAS, 444, 3592
Faedi F. et al., 2011, A&A, 531, A40
Gaudi B. S., Winn J. N., 2007, ApJ, 655, 550
Gillon M. et al., 2013, A&A, 552, A82
Hartman J. D. et al., 2015a, AJ, 149, 166
Hartman J. D. et al., 2015b, AJ, 150, 168
Hébrard G. et al., 2013, A&A, 549, A134
Hébrard G. et al., 2014, A&A, 572, A93
Hellier C. et al., 2009, Nature, 460, 1098
Hellier C. et al., 2012, MNRAS, 426, 739
Hellier C. et al., 2014, MNRAS, 440, 1982
Hellier C. et al., 2015, AJ, 150, 18
Joshi Y. C. et al., 2009, MNRAS, 392, 1532
Lendl M. et al., 2012, A&A, 544, A72
Mancini L. et al., 2014, A&A, 568, A127
Maxted P. F. L. et al., 2011, PASP, 123, 547
Maxted P. F. L., Serenelli A. M., Southworth J., 2015a, A&A, 575, A36
Maxted P. F. L., Serenelli A. M., Southworth J., 2015b, A&A, 577, A90
Maxted P. F. L. et al., 2016, A&A, 591, A55
Mayor M. et al., 2003, The Messenger, 114, 20
Pollacco D. L. et al., 2006, PASP, 118, 1407
Poppenhaeger K., Wolk S. J., 2014, A&A, 565, L1
Serenelli A. M., Bergemann M., Ruchti G., Casagrande L., 2013, MNRAS, 429, 3645
Sestito P., Randich S., 2005, A&A, 442, 615
Sing D. K. et al., 2016, Nature, 529, 59
Smalley B. et al., 2011, A&A, 526, A130
Smith A. M. S. et al., 2012, AJ, 143, 81
Socrates A., 2013, preprint (arXiv:1304.4121)
Socrates A., Katz B., Dong S., 2012, preprint (arXiv:1209.5724)
Southworth J., 2011, MNRAS, 417, 2166
Stevenson K. B. et al., 2016, PASP, 128, 094401
Triaud A. H. M. J. et al., 2010, A&A, 524, A25
Triaud A. H. M. J. et al., 2013, A&A, 551, A80
Weiss A., Schlattl H., 2008, Ap&SS, 316, 99
Winn J. N. et al., 2010, ApJ, 718, 575
Zacharias N., Finch C. T., Girard T. M., Henden A., Bartlett J. L., Monet D. G., Zacharias M. I., 2013, AJ, 145, 44

APPENDIX A: RADIAL VELOCITIES

Table A1. Radial velocities.

BJD – 2400 000 (UTC)	RV (km s^{-1})	σ_{RV} (km s^{-1})	Bisector (km s^{-1})
WASP-130			
56715.83348	1.3460	0.0065	−0.0282
56718.84774	1.4386	0.0063	−0.0140
56723.84644	1.5129	0.0072	−0.0320
56725.73618	1.4049	0.0075	−0.0361
56726.67716	1.3829	0.0076	−0.0882
56773.77647	1.3618	0.0107	−0.0173
56776.76305	1.4474	0.0067	0.0037
56778.76460	1.5612	0.0097	−0.0311
56779.70963	1.5670	0.0065	−0.0238
56803.66375	1.5488	0.0106	0.0160
56808.72754	1.3549	0.0095	−0.0595
56810.69012	1.4195	0.0085	−0.0280
56811.67572	1.4753	0.0072	0.0015
56833.65206	1.4397	0.0092	−0.0070
56837.60754	1.5885	0.0100	−0.0266
56853.59045	1.3982	0.0123	−0.0281
56879.53529	1.4451	0.0132	−0.0495
57017.84985	1.4195	0.0075	−0.0481
57031.82387	1.5514	0.0078	−0.0306
57044.82648	1.6247	0.0076	0.0136
57071.81936	1.4552	0.0076	−0.0389
57082.85670	1.4949	0.0075	−0.0088
57188.55692	1.4048	0.0112	−0.0578
57189.66971	1.3880	0.0109	−0.0189
57406.84526	1.4635	0.0090	−0.0094
57426.81680	1.5852	0.0058	−0.0316
57453.72114	1.4143	0.0051	−0.0416
WASP-131			
56694.86288	−19.6343	0.0055	0.0340
56713.72539	−19.6948	0.0071	0.0276
56723.89584	−19.6926	0.0063	0.0166
56724.87344	−19.6800	0.0058	0.0354
56726.70668	−19.6420	0.0057	0.0422
56744.91236	−19.6899	0.0059	0.0347
56745.85830	−19.6902	0.0061	0.0186
56746.62422	−19.6705	0.0061	0.0149
56748.84647	−19.6348	0.0059	0.0442
56749.72097	−19.6652	0.0054	0.0173
56769.58299	−19.6365	0.0056	0.0183
56809.72416	−19.6991	0.0058	0.0322
56810.71410	−19.6629	0.0072	0.0371
56811.72508	−19.6332	0.0070	0.0233
56830.66400	−19.6960	0.0064	0.0280
56839.62346	−19.6526	0.0067	0.0218
56864.52557	−19.6406	0.0056	0.0354
57055.82138	−19.6531	0.0059	0.0170
57071.84521	−19.6406	0.0065	0.0135
57110.88171	−19.6367	0.0077	0.0145
57139.77294	−19.6875	0.0085	0.0156
57194.63654	−19.6207	0.0080	0.0252
57458.77449	−19.6801	0.0055	0.0431
WASP-132			
56717.73665	31.1460	0.0103	0.0087
56749.88330	31.0358	0.0111	0.0298
56772.83833	31.0369	0.0099	0.0359
56779.80482	31.0630	0.0130	−0.0239
56781.68823	31.1323	0.0116	−0.0406
56782.75296	31.1388	0.0107	0.0058
56803.73759	31.0888	0.0232	0.0482
56808.75158	31.0784	0.0157	0.0360
56810.73750	31.1109	0.0153	0.0722
56811.69973	31.0846	0.0132	0.0369
56813.73159	31.0472	0.0281	0.0266
56814.74102	31.0197	0.0139	−0.0298
56830.68796	31.0877	0.0141	0.0027
56833.58020	31.0764	0.0133	0.0523
56840.60592	31.0667	0.0196	0.0671
56853.53751	31.1467	0.0504	0.0238
56855.61273	31.0228	0.0127	0.0198
56856.59422	31.0223	0.0105	0.0341
56880.53254	31.0585	0.0151	−0.0006
56888.54232	31.0888	0.0133	0.0140
56889.52621	31.0884	0.0110	0.0412
56910.48465	31.0966	0.0222	0.0143
57031.85994	31.0528	0.0150	0.0006
57072.87336	31.0326	0.0118	−0.0502
57085.80107	30.9265	0.0128	−0.0155
57086.74260	30.9483	0.0131	−0.0098

Table A1 – *continued*

Table A1 – *continued*

BJD – 2400 000 (UTC)	RV (km s^{-1})	σ_{RV} (km s^{-1})	Bisector (km s^{-1})
57111.67974	30.9845	0.0173	0.0246
57112.85851	30.9697	0.0291	−0.0224
57114.83854	30.9679	0.0212	−0.0530
57139.68574	31.0283	0.0215	−0.0124
57194.67667	31.0018	0.0278	−0.0526
57405.83694	30.9468	0.0130	−0.0141
57412.84526	30.9293	0.0176	−0.0042
57426.84822	30.9744	0.0103	0.0005
57428.82227	30.9898	0.0084	−0.0045
57455.88964	30.9471	0.0127	−0.0609
WASP-139: CORALIE			
54763.67767	−13.0496	0.0201	0.0220
54766.72371	−13.0095	0.0157	−0.0082
54776.79057	−12.9875	0.0254	0.0412
56211.82564	−12.9931	0.0143	−0.0039
56220.76495	−13.0409	0.0129	−0.0270
56516.89696	−13.0298	0.0145	0.0481
56577.69538	−13.0346	0.0114	0.0167
56578.87291	−12.9959	0.0105	0.0434
56581.87217	−13.0236	0.0101	0.0045
56623.78855	−13.0314	0.0111	0.0041
56629.59554	−13.0451	0.0116	−0.0148
56873.90932	−13.0314	0.0189	0.0315
56874.84054	−12.9882	0.0137	−0.0056
56876.88875	−13.0143	0.0148	0.0299
56877.79318	−13.0013	0.0168	−0.0149
56879.89171	−12.9778	0.0143	0.0597
56952.66033	−12.9785	0.0170	0.0036
56987.55377	−12.9923	0.0413	0.0157
56988.58979	−12.9637	0.0170	−0.0202
57038.59542	−12.9972	0.0184	0.0707
57085.52067	−13.0019	0.0154	0.0112
57286.88716	−13.0439	0.0340	−0.0055
57336.69857	−13.0050	0.0302	−0.0803
57367.71629	−12.9748	0.0168	−0.0425
WASP-139: HARPS			
56927.79489	−12.9888	0.0064	−0.0186
56929.83816	−12.9931	0.0058	−0.0043
56948.67436	−13.0052	0.0057	0.0002
56949.65985	−13.0067	0.0062	0.0179
56951.74760	−12.9814	0.0037	0.0021
56952.74043	−12.9857	0.0041	−0.0181
56953.76702	−12.9860	0.0034	0.0121
56955.70180	−13.0079	0.0029	0.0066
56957.86492	−12.9971	0.0097	−0.0048
56958.72499	−12.9856	0.0050	0.0157
56959.70035	−12.9962	0.0044	0.0032
56959.71448	−12.9984	0.0048	0.0080
56959.72874	−12.9900	0.0043	0.0126
56959.74518	−12.9994	0.0034	0.0066
56959.76257	−12.9952	0.0048	0.0093
56959.78116	−12.9929	0.0046	0.0014
56959.79786	−12.9955	0.0047	0.0101
56959.81611	−12.9907	0.0054	−0.0037
56959.83386	−12.9970	0.0057	0.0112
56959.85175	−12.9952	0.0060	−0.0198
56959.86897	−13.0020	0.0067	0.0217
56997.70376	−13.0057	0.0039	0.0043
56999.72988	−12.9820	0.0039	0.0058
57032.61218	−13.0151	0.0055	−0.0028
57033.58272	−12.9941	0.0083	0.0073
57034.60223	−12.9789	0.0062	0.0048
57035.58562	−12.9898	0.0055	0.0182

Table A1 – *continued*

BJD – 2400 000 (UTC)	RV (km s^{-1})	σ_{RV} (km s^{-1})	Bisector (km s^{-1})
WASP-140			
56920.76077	2.5349	0.0098	0.0133
56930.82132	1.7340	0.0078	0.0621
56931.82218	2.5133	0.0072	0.0327
56936.79830	2.3340	0.0080	−0.0200
56950.84894	1.7484	0.0075	0.0393
56953.78131	2.1478	0.0094	0.0583
56955.77226	1.8930	0.0080	−0.0048
56956.82473	2.4086	0.0108	0.0331
56959.76870	1.7695	0.0083	0.0436
56965.86872	2.3001	0.0075	0.0341
56978.70617	2.5095	0.0120	0.0083
56979.66055	1.9375	0.0122	0.0167
56980.76045	2.3070	0.0108	0.0344
56983.78948	2.2687	0.0101	−0.0310
56984.69862	1.7913	0.0094	−0.0291
56987.58015	2.4201	0.0165	0.0227
57004.59553	1.7625	0.0100	−0.0143
57019.69293	2.1414	0.0129	0.0144
57039.60065	2.3649	0.0105	0.0533
57060.61575	1.7552	0.0100	0.0184
57085.55015	1.9915	0.0094	0.0263
57339.77164	1.8358	0.0124	0.0171
57369.68260	2.1369	0.0230	0.0419
WASP-141			
56955.84534	34.1669	0.0320	0.0300
56965.81124	34.1291	0.0208	−0.0239
56990.59092	33.5216	0.0406	0.0124
56993.81477	33.5438	0.0472	−0.0758
57011.63059	33.9947	0.0268	0.0174
57012.68022	33.9561	0.0401	0.0222
57014.72766	33.8971	0.0300	0.0412
57016.66733	33.6264	0.0293	−0.0376
57033.72918	33.4964	0.0310	0.0756
57039.62726	33.7132	0.0392	−0.0572
57040.67281	33.5825	0.0376	0.0010
57041.67337	34.1062	0.0497	0.0222
57065.65032	34.0360	0.0361	0.0875
57118.48484	34.0519	0.0695	0.0801
57291.83917	33.5517	0.1031	0.1949
57319.74513	34.0872	0.0708	−0.1402
57333.80278	33.9814	0.0534	−0.0012
57371.75720	33.6182	0.0412	−0.0456
WASP-142			
56744.53717	47.2374	0.0201	0.0793
56747.54086	47.0456	0.0262	0.0789
56771.61011	47.1023	0.0260	0.0468
56772.58229	47.0722	0.0258	0.0260
56779.61261	47.2061	0.0321	−0.0846
56803.51322	47.1629	0.0277	0.0273
56987.86072	46.9854	0.0584	−0.1158
56996.81308	47.1962	0.0423	0.0225
57018.73174	47.0535	0.0390	0.0523
57022.76169	46.9974	0.0330	0.0288
57026.86587	46.9604	0.0300	0.0346
57043.67305	47.1643	0.0568	−0.0103
57070.67363	47.2080	0.0326	0.0080
57072.63982	47.2065	0.0425	−0.0156
57402.72844	47.0586	0.0499	−0.0392
57432.63093	47.1446	0.0269	0.0052

Bisector errors are twice RV errors.

This paper has been typeset from a TEX/LATEX file prepared by the author.